Preprints of the 21st IFAC World Congress (Virtual)
Berlin, Germany, July 12-17, 2020

Mechatronics applications of condition monitoring using a statistical change detection method

M. Mazzoleni *, **M. Scandella** *, **L. Maurelli** *, **F. Previdi** *

* *Department of Management, Information and Production engineering University of Bergamo, via Galvani 2, 24044 Dalmine (BG), Italy (e-mail: mirko.mazzoleni@unibg.it).*

Abstract: In this paper, we propose the use of a change detection strategy to perform condition monitoring of mechanical components. The method looks for statistical changes in the distribution of features extracted from raw measurements, such as Root Mean Square or Crest Factor indicators. The proposed method works in a batch fashion, comparing data from one experiment to another. When these distributions differ by a specified amount, a degradation score is increased. The approach is tested on three experimental applications: (i) an Electro-Mechanical Actuator (EMA) employed in flight applications, where the focus of the monitoring is on the ballscrew transmission; (ii) a CNC workbench, where the focus is on the vertical shaft bearing, (iii) an industrial EMA with focus on the ballscrew bearing. All components have undergone a severe experimental degradation process, that ultimately led to their failure. Results show how the proposed method is able to assess component degradation prior to their failure.

Keywords: Predictive maintenance; condition monitoring; actuators; bearings.

1. INTRODUCTION

Condition monitoring and predictive maintenance are some of the new applications enabled by the industry 4.0 paradigm, see Lamnabhi-Lagarrigue et al. (2017). Classical fault diagnosis schemes have been studied in control with a model-based focus, Varga (2017). However, data-driven methods, while more computationally demanding and less interpretable, are easier to understand and deploy, especially with many variables to manage, see Ding (2014).

Amongst the data-driven approaches, statistical change detection methods have been recently employed in condition monitoring with simulated Kammammettu and Li (2019) and experimental data Mazzoleni et al. (2018a,b). The aim is to identify when the statistical features of the data are changing, by estimating two data distributions: one before and one after a certain time instant. Change-point detection methods are usually classified into real-time, Garnett et al. (2009), and retrospective detection, Yamanishi and Takeuchi (2002), with the first methodologies giving immediate response and the second ones ensuring greater accuracy. In particular, authors in Mazzoleni et al. (2018b) proposed a condition monitoring approach based on *batch change detection* that relies on the RuLSIF technique of Liu et al. (2013), whose aim is to estimate the *ratio* of the two distributions, rather than estimating the single ones.

In this work, we *test the condition monitoring approach based on the batch change detection* on three *experimental setups*: (i) monitoring of the ballscrew transmission of an ElectroMechanical Actuator (EMA) for flight applications; (ii) monitoring of a rolling bearing in a workbench center; (iii) monitoring of a rolling bearing in an industrial EMA.

The *first activity* is carried out in the Reliable Electromechanical actuator for PRImary SurfacE with health monitoring (REPRISE) H2020 project. A description of the project and results on the *first experimental campaign* are reported in Mazzoleni et al. (2019); Mazzoleni et al. (2017b); Previdi et al. (2018) where the batch monitoring approach was introduced. To validate the method, *a second test campaign* has been conducted on a new EMA (similar to the one used during the first test phase) until its failure. Monitoring mechanical components in a EMA using data-driven methods is not a new problem, see e.g. Chirico and Kolodziej (2014); Tsai et al. (2014); Mazzoleni et al. (2014, 2017a). However, apart from previous work of the authors, as far as we are aware, change detection methods have never been applied for this purpose.

The *second activity* regards the monitoring of a rolling bearing, used in the transmission of the vertical shaft of a workcenter machine. Bearing diagnostics is a well-known problem: however, much of the research has devoted its attention to detect and isolate *local* faults (e.g. inner/outer race faults), for which common tested approaches are available, see Randall and Antoni (2011). In our case, we are instead interested in bearing degradation, for which *it is not possible to predict if a local fault will emerge*. For this reason, it is interesting to evaluate how the proposed approach performs on this task.

A similar problem is faced in the *third activity*, where the focus is on the monitoring of a rolling bearing in an industrial EMA with ballscrew transmission.

Summarizing, the contributions of this work are: (i) validate the monitoring approach, proposed in Mazzoleni et al. (2018b) by the authors, on a *second new experimental campaign* performed on the REPRISE flight EMA; (ii) evaluate the approach on *different experimental settings*, based on the monitoring of industrial rolling bearings.

2. STATISTICAL CHANGE DETECTION

The proposed monitoring algorithm is based on a density-ratio estimation method known as *Relative unconstrained Least-Squares Importance Fitting* (RuLSIF) Kanamori et al. (2009); Liu et al. (2013). The aim of the method is to *estimate the ratio of two densities*. The estimate is then used to assess how the two densities differ, using a suitable divergence. In our setting, the two densities represent kernel estimates of the time series data distribution, before and after a certain time instant.

The RuLSIF algorithm was originally designed for *on-line change detection*, i.e. assess the distribution properties *continuously* as new data arrive. In the following, we briefly review: (i) the standard on-line approach; (ii) the *batch* approach proposed in Mazzoleni et al. (2018b). Although both approaches can be employed for condition monitoring, the batch variant presents some advantages: (i) it permits to have a different number of observations in the compared experiments; (ii) it has one less hyper-parameter to tune; (iii) it allows for better detection, by comparing current data with a "reference" data set.

2.1 On-line approach

Problem statement Let $\mathbf{y}(t) \in \mathbb{R}^{d\times 1}$ be a d-dimensional time-series sample at time t. Let

$$\mathbf{z}(t) \equiv \left[\mathbf{y}(t)^\top, \mathbf{y}(t+1)^\top, \cdots, \mathbf{y}(t+k-1)^\top\right]^\top \in \mathbb{R}^{d\cdot k\times 1}$$

be a subsequence of time-series of length k, at time t. The dk-th dimensional vector $\mathbf{Y}(t)$ defines *a single data sample*. Let

$$\mathbf{Y}(t) \equiv [\mathbf{z}(t),\, \mathbf{z}(t+1),\, \cdots,\, \mathbf{z}(t+n-1)] \in \mathbb{R}^{d\cdot k\times n},$$

be the matrix composed by n of the dk-th dimensional samples $\mathbf{z}(t)$. Consider two consecutive segments $\mathbf{Y}(t)$ and $\mathbf{Y}(t+n)$. The change-detection problem is then solved by computing a certain dissimilarity measure between the data sets $\mathbf{Y}(t)$ and $\mathbf{Y}(t+n)$. The higher the dissimilarity measure is, the more likely the two distributions differ.

Dissimilarity measure The considered dissimilarity measure is the α-relative Pearson divergence measure, introduced in Liu et al. (2013). For $0 \le \alpha < 1$, we have:

$$\mathrm{PE}_\alpha\left(p\|\tilde{p}\right) \equiv \frac{1}{2}\int \tilde{p}_\alpha(\mathbf{x}) \cdot \left(\frac{p(\mathbf{x})}{\tilde{p}_\alpha(\mathbf{x})} - 1\right)^2 d\mathbf{x}, \qquad (1)$$

where $\mathbf{x}$ denotes the generic dk-th dimensional random variable, $\tilde{p}_\alpha(\mathbf{x}) = \alpha p(\mathbf{x}) + (1-\alpha)\,\tilde{p}(\mathbf{x})$ is the *α-mixture density* and $p(\mathbf{x})$, $\tilde{p}(\mathbf{x})$ are the probability density functions of the data in $\mathbf{Y}(t)$ and $\mathbf{Y}(t+n)$, respectively. The *α-relative density-ratio* is then defined as:

$$r_\alpha(\mathbf{x}) = \frac{p(\mathbf{x})}{\tilde{p}_\alpha(\mathbf{x})} = \frac{p(\mathbf{x})}{\alpha p(\mathbf{x}) + (1-\alpha)\,\tilde{p}(\mathbf{x})}, \qquad (2)$$

which it is bounded above by $1/\alpha$ for $\alpha > 0$. Equation (1) is not a metric, since it is not symmetric and the triangular inequality does not hold. To cope with the first problem, authors in Liu et al. (2013) proposed to use the symmetrical divergence:

$$\pi \equiv \mathrm{PE}_\alpha\left(p\|\tilde{p}\right) + \mathrm{PE}_\alpha\left(\tilde{p}\|p\right), \qquad (3)$$

where each term is estimated separately.

Learning algorithm The main observation of the RuLSIF change detection method is that it is easier to estimate the ratio of two densities with respect to estimating the individual ones, see Liu et al. (2013). Let $\{\mathbf{z}_i\}_{i=1}^n$ and $\{\tilde{\mathbf{z}}_j\}_{j=1}^n$ be sets of samples drawn from $p(\mathbf{x})$ and $\tilde{p}(\mathbf{x})$, respectively. The *α-relative density-ratio* (2) is modeled as:

$$g\left(\mathbf{x};\boldsymbol{\theta}\right) \equiv \sum_{l=1}^{n} \theta_l \cdot k\left(\mathbf{x}, \mathbf{z}_l\right), \qquad (4)$$

where $\boldsymbol{\theta} = [\theta_1, \ldots, \theta_n]^\top \in \mathbb{R}^{n\times 1}$ are unknown parameters, $k\left(\cdot,\cdot\right)$ is a kernel basis function with hyperparameters vector $\boldsymbol{\eta}$, and $\mathbf{z}_l$ refers to the l-th data sample in $\mathbf{Y}(t)$ (which we assume it was drawn from $p(\mathbf{x})$). The parameters vector $\boldsymbol{\theta}$ is estimated as in Liu et al. (2013):

$$\widehat{\boldsymbol{\theta}} = \underset{\boldsymbol{\theta}\in\mathbb{R}^n}{\arg\min}\left[\frac{1}{2}\boldsymbol{\theta}^\top\widehat{\mathbf{H}}\boldsymbol{\theta} - \widehat{\mathbf{h}}^\top\boldsymbol{\theta} + \frac{\lambda}{2}\boldsymbol{\theta}^\top\boldsymbol{\theta}\right], \qquad (5)$$

where $\widehat{\mathbf{H}} \in \mathbb{R}^{n\times n}$, $\widehat{\mathbf{h}} \in \mathbb{R}^{n\times 1}$ and $\lambda \in \mathbb{R}_{>0}$ controls the regularization strength. The element in position (l,m) of $\widehat{\mathbf{H}}$ is given by: $\widehat{H}_{(l,m)} = \frac{\alpha}{n}\sum_{i=1}^n k(\mathbf{z}_l,\mathbf{z}_i)\cdot k(\mathbf{z}_i,\mathbf{z}_m) + \frac{1-\alpha}{n}\sum_{j=1}^n k(\mathbf{z}_l,\tilde{\mathbf{z}}_j)\cdot k(\tilde{\mathbf{z}}_j,\mathbf{z}_m)$. The element in position l of $\widehat{\mathbf{h}}$ is given by: $\widehat{h}_{(l)} = \frac{1}{n}\sum_{i=1}^n k(\mathbf{z}_i,\mathbf{z}_l)$.

The solution in (5) can be found by minimizing the following cost: $J(\boldsymbol{\theta}) = \frac{1}{2}\int p'_\alpha(\mathbf{X})\Big(r_\alpha(\mathbf{X}) - g(\mathbf{X};\boldsymbol{\theta})\Big)^2 d\mathbf{X}$.

Computing the divergence Substituting the estimator (4) in (1) leads to the following approximation of the α-relative divergence: $\widehat{\mathrm{PE}}_\alpha = \frac{1}{2n}\sum_{i=1}^n g\left(\mathbf{z}_i;\,\widehat{\boldsymbol{\theta}}\right) - \frac{1}{2}$. The final divergence score, as reported by (3), is:

$$\widehat{\pi} \equiv \widehat{\mathrm{PE}}_\alpha(p\|\tilde{p}) + \widehat{\mathrm{PE}}_\alpha(\tilde{p}\|p). \qquad (6)$$

2.2 Batch approach

As stated previously, in Mazzoleni et al. (2018b) we proposed to use the RuLSIF method in a batch mode. The batch variant applies the RuLSIF algorithm by directly *comparing two batches of data at a time*, with the aim of evaluating how much these two data sets differ.

We denote the first dataset with n_1 observation and probability density function p as $\mathbf{Y}_1 \in \mathbb{R}^{d\cdot k\times n_1}$, and the second data set with probability density function $\tilde{p}$ as $\mathbf{Y}_2 \in \mathbb{R}^{d\cdot k\times n_2}$. The parameter k maintains its previous role. The computation discussed previously remains the same, with the proper dimensions taken into account. In both continuous and batch variant, we indicate the appropriate set of hyperparameters of the method (kernel function k hyperparameters vector $\boldsymbol{\eta}$, the regularization strength λ, k and n) with the vector $\boldsymbol{\psi}$.

The approach for computing a condition monitoring indicator is as in Mazzoleni et al. (2018b) and summarized in Algorithm 1. Let $\mathbf{Y}_\tau \in \mathbb{R}^{d\cdot k\times n}$ be the data of the test τ,

and suppose for simplicity that all tests have n observations. First, in the set-up phase, compute the divergence $\widehat{\pi}_1$ between two healthy tests, i.e. $\mathbf{Y}_0$ and $\mathbf{Y}_1$. Then, set a threshold ξ that is higher than $\widehat{\pi}_1$ but lower than 2α (the maximum value of (6)). The subsequent tests are compared with the *last experiment* $\tau = \tau^*$ *that exceeded the threshold* ξ. We call this *Last-Change policy* (see Mazzoleni et al. (2018b) for a comparison of different policies). Each time ξ is violated, a damage counter ζ_τ is incremented. The damage counter ζ_τ is taken as a *monotonic indicator of system degradation.*

Algorithm 1 Condition monitoring algorithm based on batch change detection

Input: $\mathbf{Y}_{\tau^*}, \mathbf{Y}_\tau$, hyperparameters $\boldsymbol{\psi} = [\alpha, \lambda, k, \boldsymbol{\eta}^\top]^\top$
Output: Damage indicator ζ_τ

Training or set-up phase (for $\tau \leq 1$):

1: compute the divergence $\widehat{\pi}_1$ between $\mathbf{Y}_0$ and $\mathbf{Y}_1$
2: set a threshold ξ s.t. $\widehat{\pi}_1 < \xi < 2\alpha$;

Test phase (for $\tau > 1$):

3: $\zeta_\tau \leftarrow 0$; $\tau^* \leftarrow 1$
4: compute the divergence $\widehat{\pi}_\tau$ between $\mathbf{Y}_{\tau^*}$ and $\mathbf{Y}_\tau$
5: **if** $\widehat{\pi}_\tau > \xi$ **then**
$\tau^* \leftarrow \tau$; $\zeta_\tau \leftarrow \zeta_{\tau-1} + 1$
6: **end if**

3. INDUSTRIAL CASE STUDIES

3.1 Flight electro-mechanical actuator monitoring

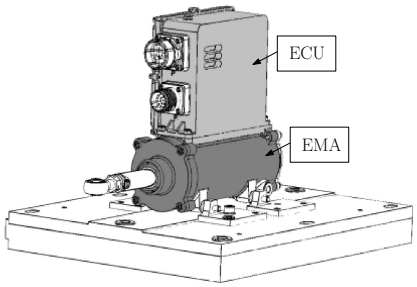

Fig. 1. EMA with its Electronic Control Unit (ECU).

The focus of the REPRISE project is on primary flight surfaces control EMAs for small aircraft. The considered EMA is a BrushLess DC (BLDC) motor with a ballscrew transmission. Part of the work is devoted to developing condition monitoring algorithms for the mechanical part of the EMA (in particular the ballscrew). A test bench has been developed to stress the EMA until failure. A schematic of the used flight EMA is shown in Figure 1.

A large experimental campaign was performed in different conditions of load and lubrication of the ballscrew. Two types of tests were conducted: (i) endurance tests; (ii) monitoring test. During endurance tests, the EMA has to overcome 800 N of load (which is higher than ballscrew specification). Monitoring tests were performed at 300 N, and data such as the motor phase currents were measured. In both test types, the EMA was commanded by *sinusoidal* position profiles, see Mazzoleni et al. (2019). One of the main possible causes of ballscrew degradation is the lack of lubricant. For this reason (and also to accelerate the EMA damaging) we tested the EMA in three different operating conditions: (i) standard level of lubricant; (ii) about half lubricant removed; (iii) lubricant completely removed.

A total of *two acquisition phases* were performed: (i) the first one from April 2018 to October 2018; (ii) the second one from February 2019 to May 2019. A thorough description of the performed tests and results *on the first acquisition phase* is presented in Mazzoleni et al. (2019); Mazzoleni et al. (2017b). In this paper, we *extend previous results based on acquisition phase 1* data (see Mazzoleni et al. (2018a,b); Previdi et al. (2018), *validating the use of Algorithm 1 on the data from acquisition phase 2*, that was specifically performed for this purpose. A review of the performed tests is reported in Figure 2. As can be seen, *both phases ended with a complete failure of the EMA*. In particular, the 2nd phase ended with a jamming of the nut-screw assembly.

In both monitoring and endurance tests of the two acquisition phases, we performed tests at 5 mm and 10 mm of sinusoidal position profile amplitude, within each one of these frequency values of the input (in Hz): $\{0.1, 0.3, 0.5, 0.8, 0.9, 1, 1.5, 2, 2.5, 4\}$, for a total of 100 periods for each frequency.

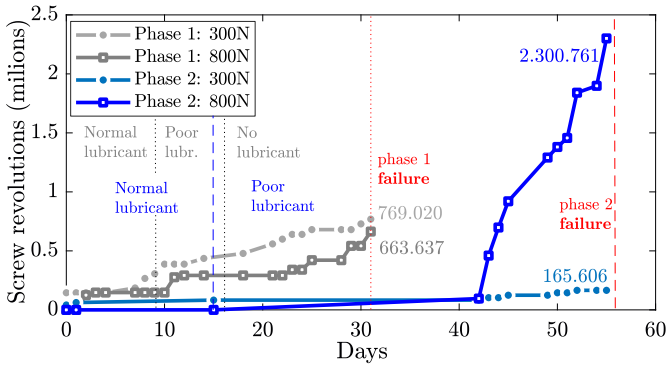

Fig. 2. Number of screw revolutions for different loads and operating conditions, in the two acquisition phases.

3.2 Bearing monitoring in high-precision workcenters

The second case study is related to the assessment of bearings degradation in high-precision workcenters. In particular, the focus is on the upper bearing of the vertical-shaft (Y direction) of a 5-axis CNC machine, see Figure 3. An endurance campaign was performed to bring the bearing to fail. The test lasted from 17 June 2019 to 27 June 2019, when the bearing underwent a complete failure. The tests consisted in vertical up/down movements of the vertical shaft, following a trapezoidal speed profile, spanning the full length of the shaft screw ($\approx$ 1300 mm). The tests were performed initially at 10 m/min of maximum speed, with poor lubricant inside the bearing. Since the 24 June 2019, we fully removed the lubricant and performed tests at 30 m/min of maximum speed, to accelerate the deterioration. During the tests, we measured the following variables for 3 s every 40 min: (i) quadrature current of the motor; (ii) motor encoder; (iii) bearing temperature; (iv) bearing vibrations. The vibrations were acquired at 12800 Hz by a tri-axial accelerometer, see Figure 4.

3.3 Bearing monitoring in industrial EMAs

This mechatronics application regards the degradation of bearings in industrial actuators. The employed EMA is a three-phase Brushless AC motor (BLAC) with ballscrew transmission. The considered bearing directly supports the screw, see Figure 5. The EMA underwent *two endurance sessions* with 1185 N load generated by a linear pneumatic motor, using trapezoidal position profiles with 150 mm amplitude, 250 mm/s speed and 2000 mm/s^2 acceleration. The endurance sessions lasted about 3 hours each. The motor traveled a total of 4.1 km with 819.000 screw revolutions. During the third endurance session, the bearing *reached a failure*. Prior to stressing the EMA, *two monitoring acquisitions* were performed, consisting of three forward/backward movements (with same settings as during endurance sessions). The monitoring acquisitions were performed after the first and the second endurance session. Measured data includes EMA position and phase currents (sampled at 10 kHz), see Figure 6.

4. CONDITION MONITORING VIA BATCH CHANGE POINT DETECTION

4.1 Flight electro-mechanical actuator monitoring

In order to employ the proposed method, it is necessary to define which data distributions are compared. The features composing $\mathbf{y}(t)$ are computed in the following way. Consider a *fixed frequency* of the sinusoidal input profile. First, computed the Root Mean Square (RMS) and the Crest Factor (CF) of the three phase currents, in each period of the input. Then, for each input period, take the average of the computed RMS and CF in that period. Thus, we have that $\mathbf{y}(t) \in \mathbb{R}^{2\times 1}$. An example of measured data is reported in Figure 7.

Results of Algorithm 1 on phase 1 monitoring data, using $k = 1, \alpha = 0.5$, and a Gaussian kernel $k(\mathbf{z}_1, \mathbf{z}_2) = \exp\left(-\|\mathbf{z}_1 - \mathbf{z}_1\|_2^2/\delta\right)$ are reported in Mazzoleni et al. (2018b, 2019) while the continuous version of Section 2.1 was presented in Mazzoleni et al. (2018a). With $k = 1$, we have that $\mathbf{z}(t) = \mathbf{y}(t)$. This means that the data

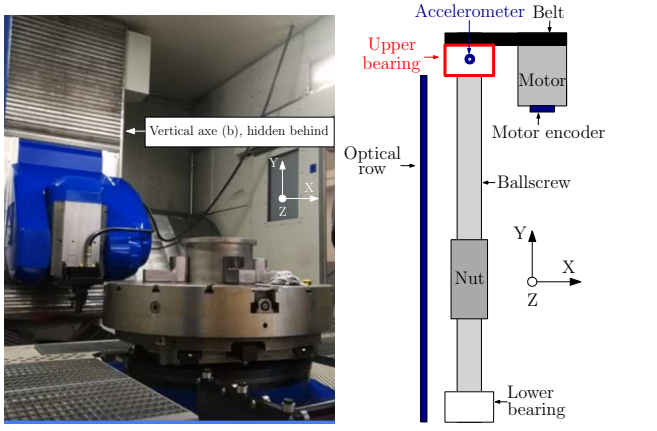

(a) The workcenter, frontal view. (b) Vertical shaft scheme.

Fig. 3. Schematic of the workcenter with upper bearing highlighted.

(a) Considered bearing. (b) Accelerometer.

Fig. 4. Bearing and accelerometer on bearing housing.

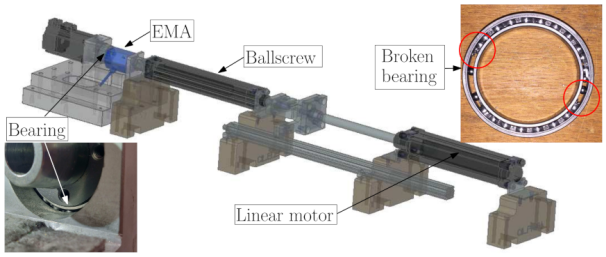

Fig. 5. Schematic of the experimental setup for the bearing monitoring of an industrial EMA.

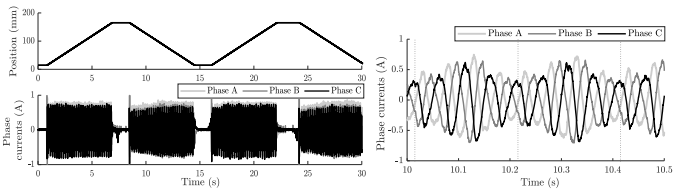

Fig. 6. Measurements from the industrial AC actuator. (Left) Test position and phase currents. (Right) Zoom on the motor phase currents. Dashed vertical lines represent a complete turn of the motor.

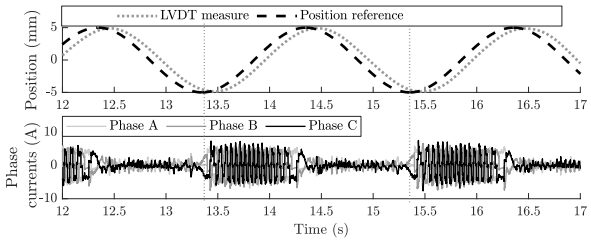

Fig. 7. Measurements from flight EMA. Vertical dashed lines indicate a period of data used to compute the RMS and CF. Frequency: 0.5 Hz. Amplitude: 10 mm. Load: 300 N.

$\mathbf{y}(t)$ are considered as independent samples: the rationale derives from the fact that each feature is computed from current data from a different and independent period of the input profile. $\mathbf{Y}(t)$ is composed by the number of sinusoidal position periods. The chosen test input profile is a sinusoid at 1 Hz frequency and 10 mm amplitude. A total of 100 periods are considered. The hyperparameters δ and λ were tuned by a cross-validation procedure (see Liu et al. (2013)), repeated for each data sets comparison.

The threshold was set to $\xi = 2 \cdot \widehat{\pi}_1 = 0.81$, such that $0 < \xi < 2\alpha = 1$.

The algorithm tuned on the 1st phase data is validated on the 2nd phase data, *with the same hyperparameters and threshold* and with the *same type of test profile* (i.e. sinusoidal input with 1 Hz frequency and 10, mm amplitude) as in phase 1. Results are reported in Figure 8. The last two experiments underwent mechanical jamming of the screw-nut assembly. For this reason, the algorithm is not able to find enough periods of the measured position profile, given by the LVDT sensor inside the EMA. In these cases, we set the RMS and CF features to 1.5 and 0.5 times their average value during the first experiment, respectively. Figure 8 depicts a zoom of the measured EMA position: it is clear how there are times where the EMA is locked in a fixed position, due to the jamming of the screw-nut assembly. Results show how the algorithm was able to detect a degradation on 08 April 2019, *about 20 days before the actuator started to jam.*

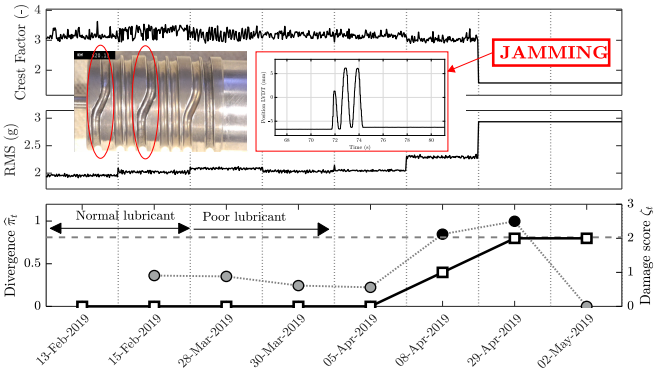

Fig. 8. Results of the proposed monitoring scheme on REPRISE phase 2 data. Damaged screw circuits and measured position due to the jam are highlighted.

4.2 Bearing monitoring in high-precision workcenters

In order to apply Algorithm 1 to the data of Section 3.3, we employed the Y-axis data of the accelerometer in Figure 4b, since it is the axis which is orthogonal to the bearing rotation. In particular, we considered the constant speed vibration data during raising motion of the Y vertical shaft of the machine (see Figure 3b). For each raising movement (from bottom to top of the machine) we computed the RMS and CF of specified vibration data, for a total of 921 features $\mathbf{y}(t) \in \mathbb{R}^{2\times 1}$. The choice of using the raising movement, with respect to the descending one, is related to the fact that, during raising direction, the structure is more stressed (the gravity does not help the motion), and therefore fault conditions are easier to assess. Here, we considered the tests on 27 June 2019. At the end of the day, *the bearing reached a failure*. An example of measured data is reported in Figure 9.

The data sets for Algorithm 1 are created as follows. As in Section 3.1, we consider $k = 1$, since each RMS and CF indicators are computed independently from each constant speed period of vibration data. Then, we subdivided the 921 features in 8 blocks, each having 115 features (we removed some features in the last block). Each block lasts

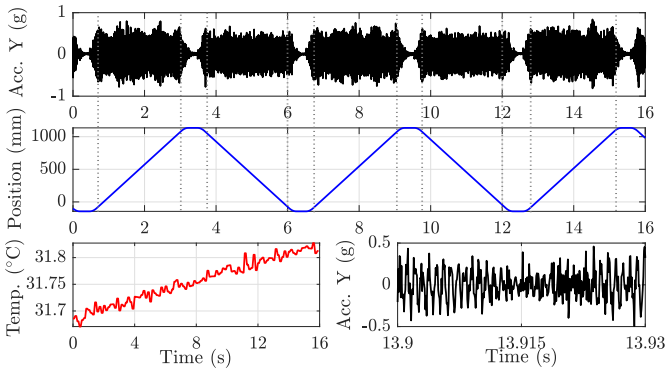

Fig. 9. Measurements from the workcenter. (Top) Bearing vibration data of Y accelerometer axis; (middle) linear vertical position; (bottom-left) temperature; (bottom-right) zoom of vibration data. Vertical dashed lines represent constant speed periods.

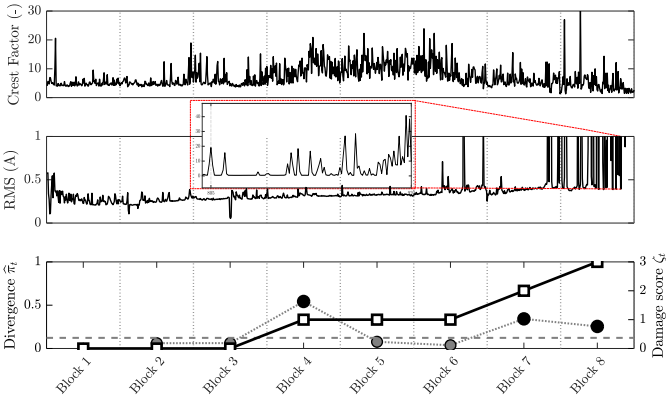

Fig. 10. Results of the proposed monitoring scheme on the workcenter bearing vibration data.

about 15 min. Then, each of these data blocks is considered as a single experiment $\mathbf{Y}_\tau$.

Results of the method, with same kernel as in Section 4.1, are shown in Figure 10, where $\xi = 2 \cdot \widehat{\pi}_1$. In the middle of bearing degradation, spikes on acceleration appear (the CF increases), while the RMS slowly increases. At the end of the day, the RMS has a huge increase that led to bearing failure. The method was able to detect the degradation *about* 45 *min before the failure.*

4.3 Bearing monitoring in industrial EMAs

As in Section 4.1, we employ the average RMS and average CF features computed from the three phase currents. Each feature is computed for each complete mechanical turn of the BLAC motor, during forwards movements. In total, there are about 70 features $\mathbf{y}(t) \in \mathbb{R}^{2\times 1}$ for each monitoring session. Again, we set $k = 1$. Thus, there are 4 experiments $\mathbf{Y}_\tau$ used to fed Algorithm 1.

Results of the method, with the same kernel as in Section 4.1, are shown in Figure 11, where $\xi = 2 \cdot \widehat{\pi}_1$. Here, the degradation trend is clearly visible from the features. The method was able to assess an anomaly *about* 16 *hours of uninterrupted working before the failure.*

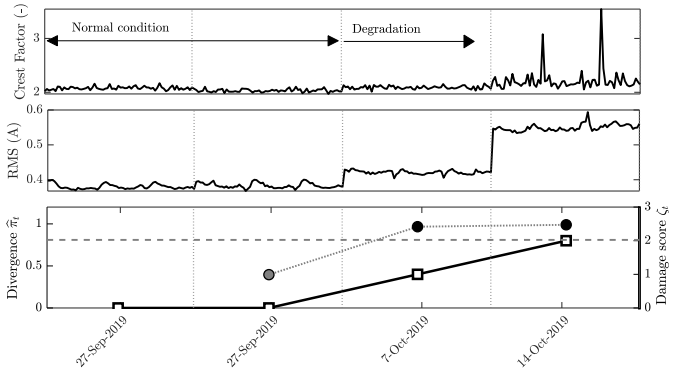

Fig. 11. Results of the proposed monitoring scheme on the bearing monitoring on the industrial EMA.

5. CONCLUSIONS AND FUTURE DIRECTIONS

In this paper, we presented a condition monitoring approach based on a statistical change detection method applied to three practical case studies from the mechatronics industry. The aim was to monitor mechanical components: a ballscrew transmission and two rolling bearings. The approach works in a batch fashion, comparing two experiments at a time, and producing a health indicator each time the distribution of features extracted from measured data of the two experiments differs by a certain amount. Results showed how the approach is able to detect degradation of the components prior to their failure. Future research is devoted to validate the method in other settings.

ACKNOWLEDGEMENTS

The flight EMA project has received funding from the the Clean Sky 2 Joint Undertaking under the European Union's Horizon 2020 research and innovation programme under grant agreement No 717112 (project acronym: REPRISE).

The workcenter project has received funding from the Italian Ministry of Economic Development (MiSE), tasks 6.1 and 6.2 of the program OR-06 2017-2020 assigned to Mandelli Sistemi SpA.

The industrial EMA project has received funding from the Lombardy region, Italy, in the context of the SMART4CPPS (Smart Solutions for Cyber-Physical Production Systems) project.

REFERENCES

Chirico, A.J. and Kolodziej, J.R. (2014). A data-driven methodology for fault detection in electromechanical actuators. *Journal of Dynamic Systems, Measurement, and Control*, 136(4), 041025.

Ding, S.X. (2014). *Data-driven design of fault diagnosis and fault-tolerant control systems*. Springer-Verlag London.

Garnett, R., Osborne, M.A., and Roberts, S.J. (2009). Sequential bayesian prediction in the presence of changepoints. In *Proceedings of the 26th Annual International Conference on Machine Learning*, 345–352. ACM.

Kammammettu, S. and Li, Z. (2019). Change point and fault detection using kantorovich distance. *Journal of Process Control*, 80, 41 – 59. doi:https://doi.org/10.1016/j.jprocont.2019.05.012.

Kanamori, T., Hido, S., and Sugiyama, M. (2009). A least-squares approach to direct importance estimation. *Journal of Machine Learning Research*, 10(Jul), 1391–1445.

Lamnabhi-Lagarrigue, F., Annaswamy, A., Engell, S., Isaksson, A., Khargonekar, P., Murray, R.M., Nijmeijer, H., Samad, T., Tilbury, D., and den Hof, P.V. (2017). Systems & control for the future of humanity, research agenda: Current and future roles, impact and grand challenges. *Annual Reviews in Control*, 43, 1 – 64. doi:https://doi.org/10.1016/j.arcontrol.2017.04.001.

Liu, S., Yamada, M., Collier, N., and Sugiyama, M. (2013). Change-point detection in time-series data by relative density-ratio estimation. *Neural Networks*, 43, 72–83.

Mazzoleni, M., Maccarana, Y., and Previdi, F. (2017a). A comparison of data-driven fault detection methods with application to aerospace electro-mechanical actuators. *IFAC-PapersOnLine*, 50(1), 12797–12802. doi:10.1016/j.ifacol.2017.08.1837. 20th IFAC World Congress.

Mazzoleni, M., Maccarana, Y., Previdi, F., Pispola, G., Nardi, M., Perni, F., and Toro, S. (2017b). Development of a reliable electro-mechanical actuator for primary control surfaces in small aircrafts. In *Advanced Intelligent Mechatronics (AIM), 2017 IEEE International Conference on*, 1142–1147. IEEE.

Mazzoleni, M., Previdi, F., Scandella, M., and Pispola, G. (2019). Experimental development of a health monitoring method for electro-mechanical actuators of flight control primary surfaces in more electric aircrafts. *IEEE Access*, 1–1. doi:10.1109/ACCESS.2019.2948781.

Mazzoleni, M., Scandella, M., Maccarana, Y., Previdi, F., Pispola, G., and Porzi, N. (2018a). Condition assessment of electro-mechanical actuators for aerospace using relative density-ratio estimation. *IFAC-PapersOnLine*, 51(15), 957 – 962. doi:https://doi.org/10.1016/j.ifacol.2018.09.070. 18th IFAC Symposium on System Identification SYSID 2018.

Mazzoleni, M., Scandella, M., Maccarana, Y., Previdi, F., Pispola, G., and Porzi, N. (2018b). Condition monitoring of electro-mechanical actuators for aerospace using batch change detection algorithms. In *2018 IEEE Conference on Control Technology and Applications (CCTA)*, 1747–1752. doi:10.1109/CCTA.2018.8511334.

Mazzoleni, M., Formentin, S., Previdi, F., and Savaresi, S.M. (2014). Fault detection via modified principal direction divisive partitioning and application to aerospace electro-mechanical actuators. In *Decision and Control (CDC), 2014 IEEE 53rd Annual Conference on*, 5770–5775. IEEE.

Previdi, F., Maccarana, Y., Mazzoleni, M., Scandella, M., Pispola, G., and Porzi, N. (2018). Development and experimental testing of a health monitoring system of electro-mechanical actuators for small airplanes. In *2018 26th Mediterranean Conference on Control and Automation (MED)*, 673–678. doi:10.1109/MED.2018.8442734.

Randall, R.B. and Antoni, J. (2011). Rolling element bearing diagnostics - a tutorial. *Mechanical Systems and Signal Processing*, 25(2), 485 – 520. doi:https://doi.org/10.1016/j.ymssp.2010.07.017.

Tsai, P., Cheng, C., and Hwang, Y. (2014). Ball screw preload loss detection using ball pass frequency. *Mechanical Systems and Signal Processing*, 48(1), 77 – 91. doi:https://doi.org/10.1016/j.ymssp.2014.02.017.

Varga, A. (2017). Solving fault diagnosis problems. *Studies in Systems, Decision and Control, 1st ed.; Springer International Publishing: Berlin, Germany.*

Yamanishi, K. and Takeuchi, J.i. (2002). A unifying framework for detecting outliers and change points from non-stationary time series data. In *Proceedings of the eighth ACM SIGKDD international conference on Knowledge discovery and data mining*, 676–681. ACM.